Surface Quantum States and Impedance Oscillations in a Weak Magnetic Field—Numerical Aspects*†

T. W. Nee, J. F. Koch, and R. E. Prange‡
University of Maryland, College Park, Maryland 20742
(Received 29 April 1968)

A numerical analysis is made of the theoretical formula for the line shape of the surface-impedance oscillations that result from microwave transitions between magnetic-field-induced surface quantum states. After some general considerations of how such calculations depend on relevant physical parameters, we present a critical comparison of the calculated and experimental curves. We illustrate how the theoretical analysis of the experimental data gives the Fermi velocity (provided the shape of the Fermi surface is known), electron mean-free time, the probability of specular reflection, all for electrons on a very small region of the Fermi surface. In addition, a parameter characteristic of the depth of penetration of the microwave electric field, namely, the skin depth δ, can be evaluated.

I. INTRODUCTION

In the presence of a magnetic field, electrons skipping along the surface of a metal by periodic specular reflection form quantum-mechanical bound states. Microwave transitions between these surface quantum states account for the oscillations of the surface impedance observed in weak magnetic fields. In a previous paper[1] the theory of such surface states has been presented together with a consideration of their contribution to the impedance in a magnetic field.

The present work is devoted to the evaluation and numerical analysis of the expressions for the surface-impedance derivative. The emphasis here is on the calculation of the line shapes of the microwave signals, and a comparison with some representative experimental data. Not only do these calculations serve as a convincing confirmation of the theory, but they also illustrate how a systematic evaluation of the experimental data gives quantitative information on Fermi-surface parameters and scattering times of the electrons.

The essential result for the surface-impedance derivative dZ/dH is contained in Eq. (39) of Ref. 1 as

$$\frac{d}{dH}Z_{xx}(H)=-\frac{ie^2}{\hbar(2\pi)^2}[Z_{xx}(0)]^2\frac{d}{dH}\times\int dk_y v_x\sum_{m,n}\frac{{\alpha_{mn}}^2}{\omega-\omega_{mn}+i\Gamma_{mn}}. \quad (1)$$

For simplicity the x direction is chosen to coincide with one of the principal axes of the impedance tensor. The magnetic field lies along the y coordinate axis and is parallel to the cylindrical sheet of the Fermi surface that contains the skipping electron states. The sample surface is the x-y plane. The integration over k_y is to be extended over the length of the Fermi surface. The quantity α_{mn} is the matrix element of the electric field $E(z)$ taken between the z-dependent factors in the wave functions for the surface quantum states, i.e.,

$$\alpha_{mn}=\frac{1}{E(0)}\int_0^\infty dz\,\Phi_n(z)E(z)\Phi_m(z). \quad (2)$$

In the denominator of the summation ω and ω_{nm} are, respectively, the experimental microwave frequency and the difference frequency $(\epsilon_m-\epsilon_n)/\hbar$ of two surface states characterized by quantum numbers m and n. The factor Γ_{mn} is equal to $\frac{1}{2}(\Gamma_m+\Gamma_n)$, where Γ_m and Γ_n represent the frequency width of the mth and nth quantum states. Aside from the rather obvious simplification of the Fermi-surface geometry, the essential approximation that has gone into the derivation of Eq. (1) is the consideration of the small signal limit; that is to say, the surface-state resonances are considered to be a small perturbation of the impedance.

There is another aspect of this calculation that is worth emphasizing. The surface-state resonances are a purely quantum-mechanical affair where the resonance frequency ω_{mn} appears as a difference in the quantum-mechanical frequencies for the bound electron states. This fact necessarily dictates the derivation of the impedance in terms of matrix elements and the Lorentzian response function, instead of the more conventional transport-equation approach. Indeed, it is readily seen, that in a classical approach to the problem, the consideration of skipping orbits would lead to resonances related to the skipping frequencies. Only in the limit of high n does the classical skipping frequency approach the quantum-mechanical beat frequency ω_{mn}.

We proceed first with a consideration of the matrix elements α_{mn} and a brief discussion of the linewidth factor Γ_{mn}. Subsequently we explore the dependence of several sample calculations on relevant physical parameters. The final section is devoted to a detailed fitting of the calculations to some characteristic experimental data, to illustrate how various physical parameters can be extracted from the data.

* Supported in part by the U. S. Air Force Office of Scientific Research (Grant No. AF-AFOSR-735-65) and the Advanced Research Projects Agency (SD101).
† Based in part on a thesis submitted by T. W. Nee to the University of Maryland in partial fulfillment of the requirements for the Ph.D. degree.
‡ National Science Foundation Senior Postdoctoral Fellow.
[1] R. E. Prange and T. W. Nee, Phys. Rev. **168**, 779 (1968).

II. MATRIX ELEMENTS AND LIFETIMES

The first step in the calculation is the consideration of the matrix elements α_{mn} as defined in Eq. (2). From this definition we see the matrix elements are a measure of the overlap of the surface-state wave functions with the electric field in the radio-frequency skin layer, and, as such, will influence decisively the amplitude and shape of the resonances. The evaluation of the matrix element for the dominant terms in the summation is done by numerical integration.

First we require the form of the electric field $E(z)$ appropriate for the anomalous skin-effect regime. For the case of specular scattering and E in a principal direction, this form appears as

$$\frac{E(z)}{E(0)}=-\frac{9}{4\pi}(1-i/\sqrt{3})\int_0^\infty \frac{x\cos(xz/\delta)}{x^3-i}dx, \qquad (3)$$

where δ is the skin depth. The simplifications made at this point are not so great as to leave substantial doubt in the final results.[2] The function $E(z)/E(0)$ is readily computed by numerical integration. Real and imaginary parts of this electric field are displayed in Fig. 1. In passing we note that, inasmuch as the characteristic depth of penetration for the skipping electrons is several δ, the formulation of $E(z)$ as in Eq. (3) is indeed quite a necessary complication. A more approximate form, such as $E(z)\propto\exp[-(1-i\sqrt{3})z/\delta]$, which is valid for small z, would lead to substantially different values for the α_{mn}.[3]

The one-dimensional wave functions $\Phi_n(z)$ for the surface states are the Airy functions. Suitably normalized, they appear as

$$\Phi_n(z)=N_n\left(\frac{2eHK}{\hbar}\right)^{1/6}\mathrm{Ai}(\zeta-\zeta_n), \qquad (4)$$

with

$$\zeta=(2eHK/\hbar)^{1/3}z \qquad (5)$$

and

$$N_n=\left[\frac{d}{d\zeta}\mathrm{Ai}(\zeta-\zeta_n)\Big|_{\zeta=0}\right]^{-1}. \qquad (6)$$

The ζ_n are successive roots of the Airy function, i.e., $\mathrm{Ai}(-\zeta_n)=0$. The factor K that enters in the definition of α represents a local radius of curvature of the Fermi surface in k space. For the detailed derivation of the equations, we refer the interested reader to Ref. 1, but to aid in visualizing these results, we sketch a few of the lower-lying states and their corresponding wave functions in the lower part of Fig. 1. These wave functions represent the periodic z-directed motion of the electrons in the triangular potential well. The magnetic field dependence of the matrix elements is contained in the field dependence of the $\Phi_n(z)$.

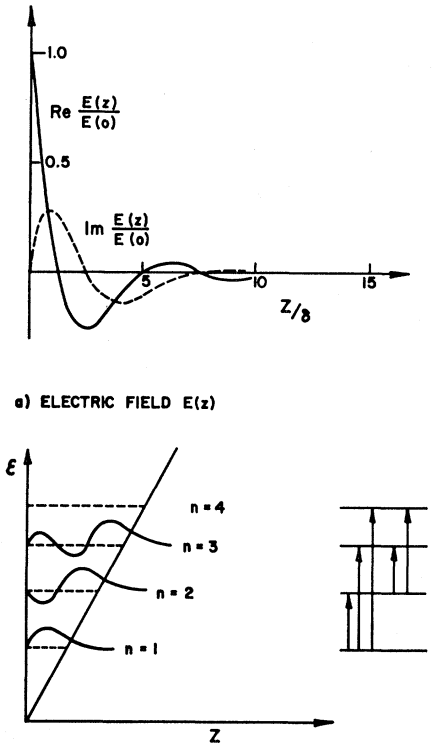

FIG. 1. Hardware used for the computation of the matrix elements α_{mn}. (a) gives the form of the electric field in the anomalous skin-effect regime. (b) is a sketch of the wave functions and energy-level scheme for electron states in a triangular potential well. Microwave transitions induced between the states (as indicated in the figure) give rise to series of spectral lines, each characterized by a given ground state.

From this point on the numerical evaluation of the α_{mn} is completely straightforward. As might be expected, the matrix elements for states confined most closely to the surface (i.e., the low-lying state $n=1$, 2, etc.) are largest in amplitude. Successively higher-order matrix elements (increasing n and m), at constant magnetic field, diminish rapidly in amplitude. This makes it possible to terminate the summation implied in Eq. (1) after a finite number of terms. The variation of the matrix elements, for fixed n and m, with changing magnetic field H is also exactly as expected. Decreasing H implies an increase in z_n, the maximal depth of penetration of the classical trajectory, and consequently a decrease in the absolute value of the matrix element.

We turn next to a consideration of the effect of the finite lifetime on the surface states. This appears in terms of a frequency width Γ_n for each of the states. The resonant response for transitions between pair states (n,m) consequently has a width proportional to

[2] Diffuse reflection is known to make a very small numerical change in the value of $E(z)$. [R. G. Chambers (private communication.)] If the current and field are not in a principal direction, some small but tedious complications ensue. We have not yet pursued the numerical aspects of this complication.

[3] T. W. Nee, Ph.D. thesis, University of Maryland, 1968 (unpublished). (This aspect, as well as many other details, are explored more fully in this thesis report.)

$\Gamma_{nm}=\frac{1}{2}(\Gamma_n+\Gamma_m)$, as implied in Eq. (1). The essential contributions to the finite lifetime are, on the one hand, phonon and impurity scattering, on the other, the possible failure of specular reflection at the metal surface because of some sort of surface roughness. This state of affairs is expressed (following the derivation in Ref. 1) by writing Γ_n as the sum of two terms

$$\Gamma_n=1/\tau+AH. \tag{7}$$

In this expression τ is the mean-free time between successive phonon or impurity scattering events, and the second term represents a "reasonable" form of surface scattering rate.[1] The constant A is independent of n and represents a measure of the surface asperity. While the linear variation of surface scattering with field is perhaps no more than an educated guess, we do consider it here in this form to illustrate how "in principle" one can extract from the data information on surface scattering. The important fact to note here is that the bulk-scattering time is independent of the magnetic field strength, whereas the surface-scattering rate has an explicit dependence on field.

III. SURFACE-IMPEDANCE CALCULATIONS

To proceed with the evaluation of the expression for the surface-impedance derivative [Eq. (1)], we make next a convenient (and not necessarily justified) simplification. Whereas, in principle, the quantities v_x, α_{mn}, ω_{mn}, and Γ_{mn} are functions of k_y, we take these as constant and equal to their value at the position on the Fermi surface where ω_{mn} has an extremal value. In practice this amounts to considering the Fermi-surface section responsible for the signals, in the form of a cylinder with constant relaxation time and Fermi velocity. To some extent this "cylindrical approximation" is justified from the experimental observation on the angular variation, polarization, and tip dependence of signals.[4] The cylindrical approximation, although not necessary in principle, makes for a significant simplification in the computations.

In order to discuss the results of our calculation in general terms, we introduce a suitably normalized magnetic field h as

$$h=H\frac{e}{\hbar}\left(\frac{v_x}{\omega(2K)^{1/3}}\right)^{3/2}, \tag{8}$$

in terms of which the resonant-field values h_{mn} are given by

$$h_{mn}=(\zeta_m-\zeta_n)^{-3/2}. \tag{9}$$

The matrix elements α_{mn} depend on the value of the magnetic field H through the surface-state wave functions $\Phi_n(z)$. They also contain the microwave skin depth δ as a parameter. We express this dependence through a quantity β defined by

$$\beta=\left(\frac{v_x}{2K\omega}\right)^{1/2}\frac{1}{\delta}. \tag{10}$$

Except for a numerical factor (approximately $\frac{1}{3}$), β represents the ratio of the maximal depth of penetration of the $n=1$ trajectory to the skin depth δ at the position of the fundamental resonance $h_{12}=0.432$. As defined in Eq. (10), β is inversely proportional to the skin depth and is independent of magnetic field. We also choose to express surface scattering by a normalized parameter

$$a=(H/h)(1/\omega)A. \tag{11}$$

With the assumption of cylindrical Fermi-surface geometry and the substitution of the normalized field coordinate and parameters, our formula for the impedance derivative now appears as

$$\frac{dZ}{dH}=\text{const}\times\frac{d}{dh}\sum_{m,n}\frac{\alpha_{mn}^2(\beta,h)\times(i-\sqrt{3})}{1-h^{2/3}(\zeta_m-\zeta_n)+i[(1/\omega\tau)+ah]}. \tag{12}$$

The phase factor in the numerator results from the usual expression for $Z(0)$ in the anomalous skin-effect regime, i.e., $Z(0)=R(0)(1-i\sqrt{3})$. The constant appearing in front of the equation is a positive real quantity. As expressed above, the impedance derivative depends on four adjustable parameters, namely, the skin-depth parameter β, the relaxation-time parameter $\omega\tau$, the surface-scattering parameter a, and the scale parameter connecting the actual magnetic field H to the normalized field h. This scale factor contains the Fermi-surface parameters K and v_F [see Eq. (8)], as well as the microwave frequency ω. The field scale parameter will not affect the line shapes or amplitudes of the resonances, but merely adjusts scales to fit the actual data.

In principle, the summation implied in Eq. (12) is extended over all possible pairs of surface states. However, in practice, the matrix elements α_{mn} decrease rapidly enough with increasing m or n to allow us to terminate the sum after a finite number of terms. To explore this convergence question we have calculated separately a number of series, each characterized by a different ground state n, as a function of h. We choose representative values of $\beta=0.5$, $\omega\tau=10$, and for simplicity take $a=0$. The results for the real part of dZ/dH appear in the first part of Fig. 2. Individual series for $n=1$, 4, and 10 are shown together with the sum over the entire 20 series, all on the same vertical scale. An examination and comparison of the individual series with the sum curve will convince the reader that the interference between series is an essential feature in the line shape, linewidth, and amplitude of the final

[4] J. F. Koch and C. C. Kuo, Phys. Rev. **143**, 470 (1966).

curve. It is apparent that the summation over 20 series yields quite a satisfactory representation of the spectrum. (The skeptical reader may take a quick glance at the experimental traces in Figs. 7 and 9.) All of the following calculations are restricted to $n \leq 20$.

We next explore the question of how the resonance condition, i.e., $h=h_{mn}$, is characterized in the dR/dH and dX/dH curves ($Z=R-iX$). To this purpose we give in Table I the resonance values of h_{mn} for some of the representative series of peaks. The position of the resonant-field values are marked as a series of arrows in Fig. 2 for both the real and imaginary parts of the surface-impedance derivative. It is readily apparent that the resonances correspond quite closely to the dR/dH maxima, or alternatively to the dX/dH zeros. A more thorough fitting and examination of this resonance criterion shows that the error incurred in the identification of the dominant high-field dR/dH peak as h_{12} amounts to about 1 or 2% for characteristic experimental curves. The true resonance is located at slightly higher fields. [The question of this deviation has been explored more fully in a thesis.[3]] It is interesting to note that the resonance criterion is much the same as for Azbel-Kaner cyclotron resonance, where the dR/dH maxima also correspond to the resonances. The present calculation provides the justification for the identification of the peaks as the relevant resonance criterion, as had been assumed plausible in previous work.[1,5]

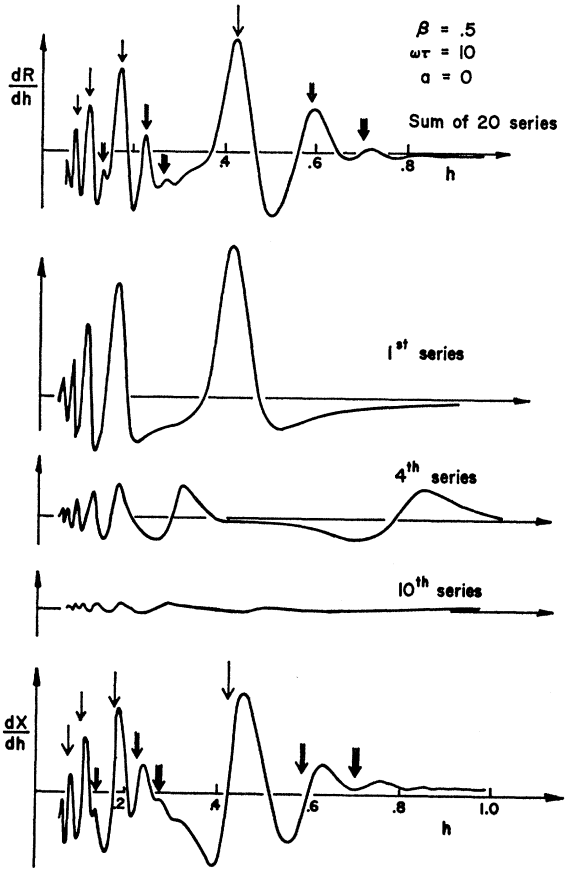

FIG. 2. Resonance spectrum for the real and imaginary parts of the impedance derivative. The resonance positions $h=h_{mn}$ are marked on the calculated curves. To illustrate the convergence of the summation for dR/dH, several individual series have been calculated. The final dR/dh and dX/dh curves represent the sum of 20 such series. (dR/dh and dX/dh amplitudes are arbitrary.)

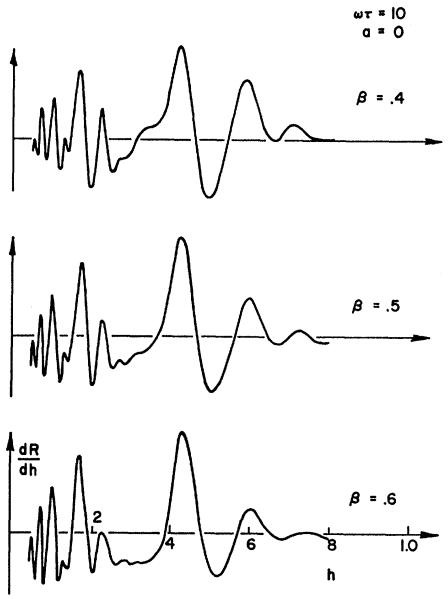

FIG. 3. Dependence of the calculated dR/dH spectrum on the skin-depth parameter β. The quantity β is inversely proportional to the skin depth δ and is approximately equal to $\frac{1}{3}$ times the ratio of the depth of penetration for the $n=1$ state to skin depth at the fundamental resonance $h_{12}=0.432$. A fit of the parameter to experimental data provides a measure of δ. The amplitude scale is arbitrary, but is identical for each of the tracings.

The skin-depth parameter β that is contained in the matrix elements will influence largely the relative amplitudes of different peaks in the oscillatory curves. With an increase in skin depth δ, and consequently smaller values of β, we expect that resonances between surface states with higher values of n, m should become more pronounced. This state of affairs is apparent in Fig. 3, where we show a sequence of curves for different values of β and fixed $\omega\tau$. We see, for example, that the

TABLE I. Resonance values of the normalized field coordinate h for the series starting with $n=1$, 2, and 3.

m	h_{m1}	h_{m2}	h_{m3}
1			
2	0.432		
3	0.176	0.583	
4	0.107	0.226	0.702
5	0.075	0.132	0.265
6	0.058	0.091	0.153
7		0.069	0.104
8			0.078

[5] T. W. Nee and R. E. Prange, Phys. Letters **25A**, 582 (1967).

peak at $h_{23}=0.583$ appears largest for $\beta=0.4$ and, subsequently, decreases in amplitude with increasing β. There is no change in the natural width of each of the resonant peaks. The apparent narrowing that occurs for the h_{12} peak is due to the decrease in the amplitude of neighboring resonances on the low-field side. Fitting values of β to experimental curves provides a direct measure of the microwave skin depth δ, if the curvature K is known for the section of Fermi surface where the signals originate. We note also that calculations based on an exponential form for $E(z)$ gave considerably less satisfactory fits to the data.[3] This result constitutes support for the theoretical shape of the penetrating microwave field as expressed in Eq. (3).

We proceed with a consideration of how the resonances depend on the value of $\omega\tau$ with fixed β. As expected, the peaks sharpen considerably and increase in amplitude as $\omega\tau$ is made larger. Additional new peaks are resolved. Nevertheless, there is only a very small shift in the position of the dR/dH maximum for the dominant resonances (such as h_{12}). The amplitudes are found to vary approximately as the square of $\omega\tau$. This is apparent from the amplitude scale on the curves of Fig. 4, which shows three calculated curves with different values of $\omega\tau$. The fit of some value of $\omega\tau$ to the experimental resonance curves gives the relaxation time for the group of electrons responsible for the resonance.

The width of the resonances depends not only on $\omega\tau$ but also on the possible lack of perfectly specular scattering at the surface. It is possible to separate out this contribution to the linewidth, because such scattering will have an explicit dependence on the value of magnetic field.[1] As in Eq. (7), we assume a linear dependence on field, with a coefficient proportional to "roughness" of the surface. Keeping fixed values of β and $\omega\tau$, we show in Fig. 5 curves computed for different values of the normalized asperity parameter a. The predominant effect to note here is that increased surface scattering reduces the amplitude and increases the width of the high-field resonances leaving the low-field peaks largely unaffected. This dependence on surface scattering is characteristically different from the variation produced with changes in $\omega\tau$ or β, and one should be able to reliably extricate a surface-scattering parameter in a fit to experiments.

Before concluding this discussion we want to return once more to the basic assumption made for these calculations, namely, the assumption of the cylindrical

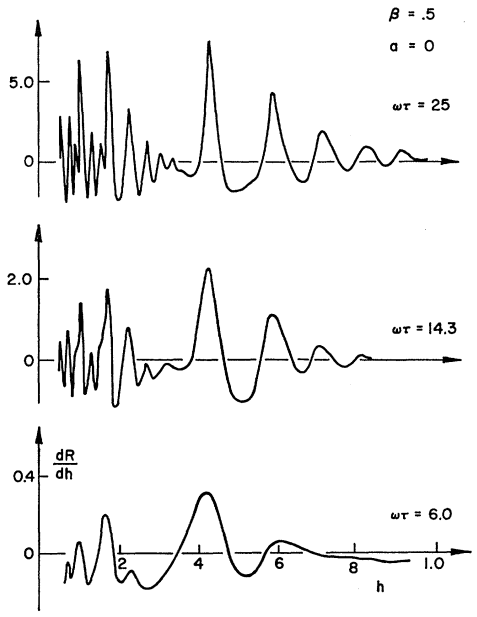

FIG. 4. Amplitude, linewidths, and the number of peaks resolved depend sensitively on $\omega\tau$. The relative amplitude for each of the curves is adjusted according to the scale marked on the figure. Fitting $\omega\tau$ to experimental data measures the relaxation time of the electrons.

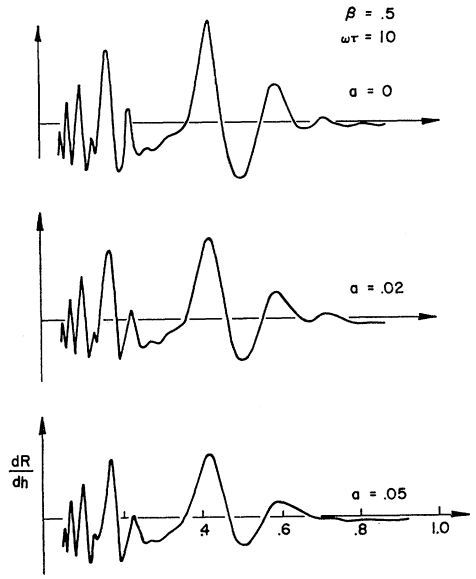

FIG. 5. Because of the lack of perfectly specular reflection at the sample surface, the resonances are broadened. The effect of increasing the surface asperity parameter is particularly noticeable at high values of field h. The amplitude scale is arbitrary, but is identical for each of the tracings.

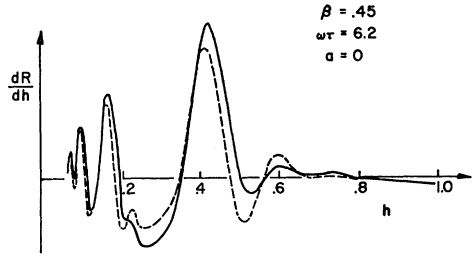

FIG. 6. If we assume that the field scale parameter is a function of position on the Fermi surface, the resultant curve (here shown as a solid line) is broadened and shows less detailed structure than the central section alone (broken line). The calculation here assumed that the extremal value of H/h is a minimum. The solid curve represents the sum over k_y slices of the Fermi surface. (Amplitude scale is arbitrary.)

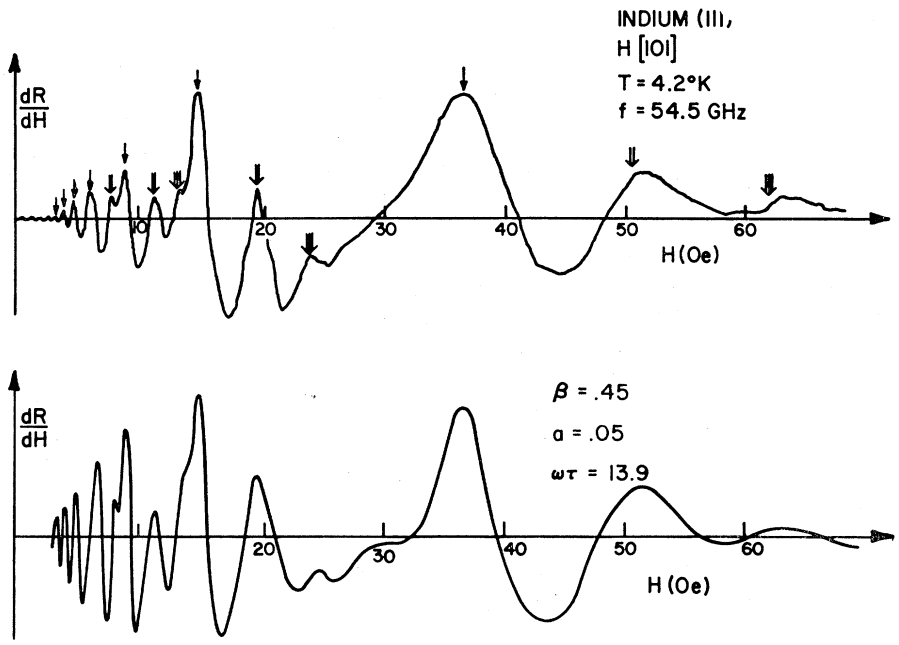

FIG. 7. Comparison of experimental and best-fit calculated curves for indium (111)-plane data at 54.5 GHz. Parameters used in the calculation are indicated on the figure. The amplitudes have been adjusted arbitrarily to appear similar in the two tracings.

Fermi surface with constant velocity and relaxation time τ. As noted earlier, although this assumption is not necessary in principle, it makes for a significant simplification of the calculations. In real metals we are not likely to encounter such very simple Fermi-surface geometry and it may well be necessary to calculate the k_y integral. The quantities α_{mn}, τ, a, and the scale factor H/h become functions of k_y. That is to say, each slice of the Fermi surface normal to the field will give its own characteristic oscillation spectrum, with the central section, say (where the parameters presumably have stationary values), dominating the resulting signal. To explore the nature of k_y broadening we have carried out such a calculation for the gently anisotropic model of an elongated ellipse (see Fig. 6). As expected, the central section makes the most important contribution, but there is a noticeable increase in linewidth, which results from the addition of signals due to neighboring sections. It is readily evident that, when there is substantial k_y broadening, the position of the peaks is shifted somewhat, and it is difficult to exactly determine the value of τ. The k_y broadening is expected to be nonsymmetric, because the extremal value of H/h will usually be either a minimum (belly-like) or maximum (neck-like), so that k_y slices neighboring the stationary one will contribute resonances at greater (lesser) field values. However, by an examination of the temperature or frequency dependence (as in the following section), it may be possible to separate unambiguously the two contributions to the linewidth. The situation with respect to k_y broadening is much the same as for the Azbel-Kaner cyclotron resonance, where m^* broadening affects both linewidth and line shapes of the resonances. We are continuing to investigate the effects of the breakdown of the cylinder approximation.

IV. COMPARISON WITH EXPERIMENTS

The preceding section was concerned with exploring the general features of the calculated curves and explicitly illustrating the dependence of these on each of the parameters that appear in the calculation. We now turn to an attempt to fit such calculated curves to the experimentally observed dR/dH oscillations by a judicious choice of the four parameters β, $\omega\tau$, a, and the scaling factor H/h. These values are then to be compared with what is known about the sample from other measurements.

We choose data taken on an indium (111)-plane sample with the magnetic field oriented along the [101] axis. In this orientation we observe a signal that is largely due to a single cylindrical section of the Fermi surface, aligned parallel to this axis. As expected for such a geometry, the peak positions move to increasing field approximately as $1/\cos\theta$, when the field is rotated away from the [101]. The data shown in the figures below are taken with the radio-frequency current perpendicular to the field and at a temperature of 4.2°K. To explore the frequency scaling of the parameters, the same sample has been run at two different frequencies, namely, 54.5 and 32.57 GHz.

Guided by the general considerations of the previous section, we have chosen various sets of values for the parameters in the calculation in an attempt to "fit" the data. The field scaling parameter H/h is readily determined by matching up peak positions in the two curves. Values of β, $\omega\tau$, and a are then chosen by trial and error to produce an aesthetically pleasing facsimile of the experimental tracing. Figure 7 shows the best fit obtained to the 54.5-GHz data using a limited number

of choices of the three parameters. The values that produce this best fit are $\beta=0.45$, $\omega\tau=13.9$, and $a=0.05$.

While the over-all agreement of calculation and experiment is satisfactory, there is nevertheless room for improvement. In particular, we note that the experimental oscillations tend to decay more rapidly at low fields, and also the high-field peaks in the experiment appear broader than the corresponding calculation. We have juggled the parameters around systematically without getting notable improvements in the fit, and the final values and parameters represent a compromise.

While the choice of an appropriate β, which determines the over-all amplitude pattern (compare Fig. 3), is not too difficult, the choice of $\omega\tau$ and a prove more troublesome. If, for example, we try to patch up the calculation to produce a more rapid decay of the very-low-field oscillations (as well as increase the width of the high-field peaks) by lowering $\omega\tau$, we lose a great deal of the structure at intermediate fields. On the other hand, the effect of raising the surface-scattering parameter a is to increase the width of the high-field peaks (because of the linear dependence on H) and leave the low-field portion unaffected. Some of that is certainly needed and our choice of the coefficient here is made to accomplish this. However, the high-field peaks are still too narrow. A further increase in a, however, will take its toll in the structure at intermediate fields (10–20 Oe). It appears that if the surface-scattering term were to depend more strongly on H, perhaps as H^2, we could produce a better fit. We have been able to reproduce accurately small, selected portions over a narrow field range by appropriate choice of Γ for each value of H. This approach gives us an empirical relation $\Gamma(H)$, that in principle should resolve the question of how surface scattering depends on field. Nevertheless, more detailed work will be necessary.

Lest we get too concerned about the remaining discrepancies, it is well to cite some of the possible reasons, both experimental and theoretical, for why it is not likely that we can do very much better. On the experimental side, there is the fact that even though the [101] signal is relatively clean, there is nevertheless another oscillatory signal mixed in. A weak signal due to another cylindrical position appears at slightly higher fields in this orientation. There may also be a small amount of magnetic field inhomogeneity over the region of the sample. Finally, in spite of our best intentions, there is some amount of overmodulation and consequent distortion of the line shape at the lowest fields. The calculations, on the other hand, neglect "k_y broadening" and use a simplified expression for $Z(H)$, especially since the [101] axis is not a principal axis of the impedance tensor in the (111) plane. The question of the k_y dependence of various quantities in the calculation is most troublesome. One expects that if the resonance parameter varies with k_y, this should make a contribution to the effective linewidth that would look somewhat like the relaxation time broadening (compare Fig. 6). In fitting a value of $\omega\tau$ in the cylindrical-model calculation, we will then not get the true electron scattering time. We also note that the predicted linear dependence of surface scattering on the magnetic field is based on an idealized model of surface roughness.

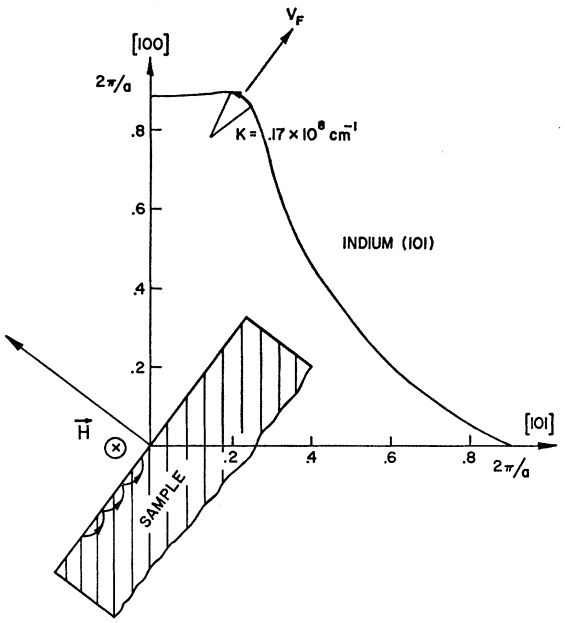

FIG. 8. Sample and Fermi-surface geometries appropriate for the (111) plane. The magnetic field is along a [101] axis and into the plane of the figure. Electrons skipping along the surface are located on a small section of the second-zone hole surface of indium. The electron in a bound surface state repeatedly traverses the narrow angular range ($\simeq1°$) as indicated.

We turn now to an examination of the values of the parameters fit in the calculation. To start with, the field scaling parameter necessary to fit peak positions is $H/h=86.4$ Oe and yields a value for K/v_F^3 of 21.7 $\times10^{-18}$ sec^3 cm^{-4}. Extensive studies of the angular anisotropy and polarization dependence of the indium plane signals[6] suggest that the [101]-axis data arises from electrons traversing the ridge of the square protuberance on the second-zone hole surface. This ridge is reasonably uniform with respect to k_y and one should expect the extremal value of K/v_F^3 to be associated with the central section of the ridge. We show the central cross section of the second-zone surface[7] in Fig. 8 and indicate the segment of electron orbit that we believe is responsible for the signal. While skipping along the metal surface, the electron repeatedly traverses this small section of the Fermi surface. The value for the local radius of curvature determined from this model is $K\approx0.17\times10^8$ cm^{-1}. The value of the Fermi velocity

[6] J. D. Jensen, Ph.D. thesis, University of Maryland, 1968 (unpublished).

[7] We are indebted to J. R. Anderson for supplying the orthogonalized-plane-wave parameters and computer program to allow us to calculate the shape of this section.

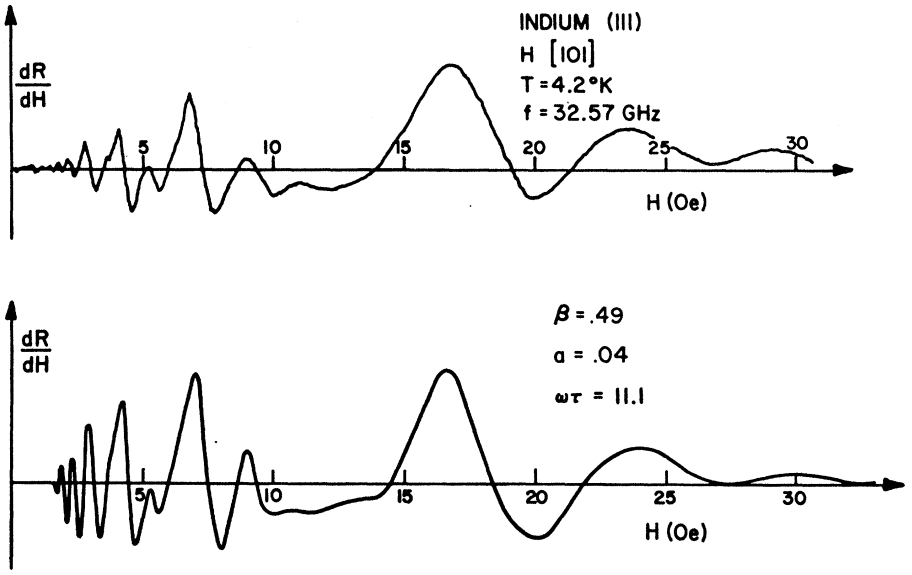

FIG. 9. Experimental and best-fit calculated curves for the indium (111)-plane data at 32.57 GHz. The amplitudes have been adjusted arbitrarily to appear similar in the two tracings.

at this point appears then as $v_F = 0.92 \times 10^8$ cm/sec. This value is well in line with velocities determined by Mina and Khaikin[8] from an analysis of cyclotron-resonance data, and gives us confidence in the over-all formulation of the surface-state problem. Recent measurements in bismuth, where the Fermi-surface shape and velocities are well established, have allowed us to make an even more critical comparison.[9]

The value of β determined from the fitting is 0.45. Using Eq. (10), we can relate this to the microwave skin depth δ. Inserting $K = 0.17 \times 10^8$ cm^{-1} yields $\delta = 0.63 \times 10^{-5}$ cm at a frequency of 54.5 GHz. This value of the skin depth is just about what we would expect, but there is not available relevant experimental evidence to make an exact comparison.

Surface scattering in the calculation is described by $a = 0.05$. The value of this parameter is much dependent on the assumed functional form of the dependence of such scattering on field. It is not very accurately determined from our calculation, to the extent that experiment and calculation do not match in all details. Nevertheless, we stress that it appears necessary to have a linewidth parameter that increases with field in order to produce a satisfactory fit to the data. The present value of a as 0.05 at a field of approximately 36 Oe (i.e., the position of the $n=1$, $m=2$ transition) implies an effective scattering rate due to lack of specularity that is 0.3 of the bulk scattering rate determined below. Expressed in terms of the probability of specular reflection [see Eq. (48), Ref. 1], this is equivalent to a value of $P = 0.88$.

The value of $\omega\tau$ derived from the calculation is 13.9. Although not unreasonable, it is considerably lower than the value we would have assigned from an examination of cyclotron-resonance signals in this specimen, i.e., $\omega\tau \simeq 30$. Because one is measuring the relaxation time on a very small portion of the Fermi surface, it is not surprising to find a value substantially different from that appropriate for an orbital average. Very likely, however, the discrepancy here results from trying to represent the linewidth as solely due to collision broadening, when indeed the k_y anisotropy makes a substantial contribution to the width. We shall explore this question further with a consideration of frequency scaling of the experiment and calculations.

In an effort to examine more critically the parameters introduced in the calculation we have repeated the indium measurements at a frequency of 32.57 GHz. The sample is remounted in the low-frequency spectrometer and we obtain the experimental curve in the upper portion of Fig. 9. Parameters β, a, and the field scaling H/h are adjusted according to their predicted dependence on frequency, whereas we allow $\omega\tau$ to vary until a satisfactory fit is obtained. The resulting calculation gives $\omega\tau = 11.1$, rather than the predicted value of 8.3 obtained by frequency-scaling $\omega\tau$. In fact, when the calculation is done using 8.3, the resulting curve gives linewidths considerably greater than the experimental tracing. A great deal of the structural detail does not appear in the calculation. It seems that there is a contribution to the linewidth parameter that does not scale linearly with frequency. This would be expected when there is k_y broadening.

V. CONCLUSIONS

We are convinced that, on the whole, the formulation of the surface-state problem and the impedance calculations are essentially correct. The comparison of calculation and experimental data provides a most convincing

[8] R. T. Mina and M. S. Khaikin, Zh. Eksperim. i Teor. Fiz. **51**, 62 (1966) [English transl.: Soviet Phys.—JETP 24, 42 (1966)].
[9] J. D. Jensen and J. F. Koch (to be published).

confirmation of the theory for the magnetic-field-induced surface quantum states.

Throughout the present work, we have aimed to illustrate how various physical parameters can be obtained from an analysis of the experimental data. Certain refinements in the calculation (as well as in the experiments) will be necessary to eventually produce a point-by-point fit of experiment and calculations. In view of remaining discrepancies, it would only be fair to emphasize that the present work is meant as an "in principle" demonstration of what one can learn. The assignment of the oscillatory signal, as due to a ridge along the Fermi surface of indium, must be considered as tentative until more exhaustive studies have been completed.

ACKNOWLEDGMENTS

We wish to thank J. D. Jensen for supplying the experimental data on the indium (111) plane that has been analyzed in this work, and acknowledge the support of the Naval Ordnance Laboratory in carrying out some of the experimental work. We thank the Computer Science Center of the University of Maryland for making available time for the numerical calculations.

PHYSICAL REVIEW VOLUME 174, NUMBER 3 15 OCTOBER 1968

Angular Forces in the Lattice Dynamics of Face-Centered Cubic Metals. II

Y. P. VARSHNI AND P. S. YUEN
Department of Physics, University of Ottawa, Ottawa 2, Canada
(Received 11 June 1968)

The lattice dynamics of the fcc lattice has been investigated with a model in which interatomic forces include, in addition to central forces, angular forces of the type suggested by de Launay. The model has been applied to copper, and results have been compared with a model investigated previously which had angular forces of the type employed by Clark, Gazis, and Wallis.

INTRODUCTION

RECENTLY, the authors[1] have investigated the lattice dynamics of fcc metals using a model in which, in addition to central forces, angular forces of the type employed by Clark, Gazis, and Wallis[2] (CGW) were included. The CGW model was applied to copper. The angular forces in this model arise from the resistance to deformation of certain angles formed by three lattice points. The change in the potential energy due to a change $\delta\theta$ in the angle θ is given by $\frac{1}{2}\kappa(\delta\theta)^2$, where κ is the angular-force constant.

de Launay[3] has considered another type of angular force which depends on the angle that the line joining the moving atoms makes with the equilibrium position of the line. The mechanical analogy is a rod connecting the particles, the rod being fastened at its ends to the equilibrium position by springs perpendicular to the rod. Hendricks, Riser, and Clark[4] have used a model that has central forces up to second neighbors and angular forces up to first neighbors to calculate the vibrational spectra and specific heats of lithium and vanadium (bcc lattice). In the present paper, we investigate a model for the fcc lattice that has central and angular forces (de Launay type) up to and including second neighbors and apply this model to copper. This model will be called the DAF (de Launay angular-force) model.[5]

DAF MODEL

We consider a monoatomic fcc lattice and represent the central-force constants for the first and second neighbors by α_1 and α_2 and the angular-force constants by σ_1 and σ_2.

As shown by de Launay,[2] the displacement that is effective for the angular-force constant σ due to displacements $\mathbf{s}_m$ and $\mathbf{s}_n$ of the particle m and particle n, respectively, is given by $\boldsymbol{\varepsilon}_{mn}\times(\mathbf{s}_n-\mathbf{s}_m)$, where $\boldsymbol{\varepsilon}_{mn}$ is the unit vector from the particle m to the particle n. Thus the change in potential energy due to $\mathbf{s}_m$ and $\mathbf{s}_n$ is

$$V_\sigma=\tfrac{1}{2}\sigma[\boldsymbol{\varepsilon}_{mn}\times(\mathbf{s}_n-\mathbf{s}_m)]^2. \quad (1)$$

Using standard methods, the secular equation for the determination of the angular frequencies ω may be derived. We merely quote here the result:

$$|D(\mathbf{q})-\omega^2MI|=0, \quad (2)$$

where M is the mass of a particle and I is the 3×3 unit matrix. The elements of the dynamical matrix $D(q)$ are as follows:

$$D_{xx}=4\alpha_1+8\sigma_1-2(\alpha_1+\sigma_1)C_1(C_2+C_3)-4\sigma_1C_2C_3+4\alpha_2S_1^2+4\sigma_2(S_2^2+S_3^2), \quad (3)$$

[1] P. S. Yuen and Y. P. Varshni, Phys. Rev. **164**, 895 (1967).
[2] B. C. Clark, D. C. Gazis, and R. F. Wallis, Phys. Rev. **134**, A1486 (1964).
[3] J. de Launay, Solid State Phys. **2**, 220 (1956).
[4] J. B. Hendricks, H. N. Riser, and C. B. Clark, Phys. Rev. **130**, 1377 (1963).
[5] Not to be confused with the better known de Launay electron-gas model.